

RT-DETRv2 Explained in 8 Illustrations

Ethan Qi Yang CHUA, Jen Hong TAN

Data Science and Artificial Intelligence Lab
Singapore General Hospital

ABSTRACT

Object detection architectures are notoriously difficult to understand, often more so than large language models. While RT-DETRv2 [1] represents an important advance in real-time detection, most existing diagrams do little to clarify how its components actually work and fit together. In this article, we explain the architecture of RT-DETRv2 through a series of eight carefully designed illustrations, moving from the overall pipeline down to critical components such as the encoder, decoder, and multi-scale deformable attention. Our goal is to make the existing one genuinely understandable. By visualizing the flow of tensors and unpacking the logic behind each module, we hope to provide researchers and practitioners with a clearer mental model of how RT-DETRv2 works under the hood.

1. INTRODUCTION

Object detection plays a critical role in computer vision, with models such as YOLO [2] achieving efficiency by framing detection as a single-pass regression task over dense anchor boxes, followed by heuristic post-processing like non-maximum suppression (NMS). While fast, these approaches often struggled with spatial context and multi-scale objects.

The introduction of DETR (DEtection TRansformer) [3] marked a shift: object detection was reformulated as a set-prediction problem, where global attention and bipartite matching directly produce object queries. Although elegant, DETR converges slowly and has difficulty with small objects due to its reliance on global attention.

RT-DETRv2 [4] was designed to overcome these limitations. It incorporates deformable attention, hybrid encoding, denoising, query-based decoding, and other refinements to achieve real-time performance without anchor heuristics. Despite these advances, the architecture of RT-DETRv2 remains complex, and existing diagrams in the literature rarely make the tensor flow or design choices easy to grasp.

In this article, we aim to demystify RT-DETRv2. Using eight carefully designed illustrations, we progressively break down the model—starting from the overall pipeline, through the encoder and decoder, and down to intricate components like multi-scale deformable attention. Our goal is not to introduce new methods, but to make an important model accessible by visualizing how its parts truly fit together.

2. METHOD

The RT-DETRv2 architecture can be divided into five main components: the CNN backbone, hybrid encoder, denoising task, query selection, and decoder. In this article, ResNet50 [5] is the CNN backbone, and we follow the default configuration described in the original paper/code in Transformers library, using input images of size (640, 640), 300 object queries, and 100 denoising bounding boxes, denoted by d from Figure 2 to 8, varies across batches. We use B to denote batch size. Figure 1 illustrates the overall tensor flow in RT-DETRv2 during inference, where the denoising task is disabled.

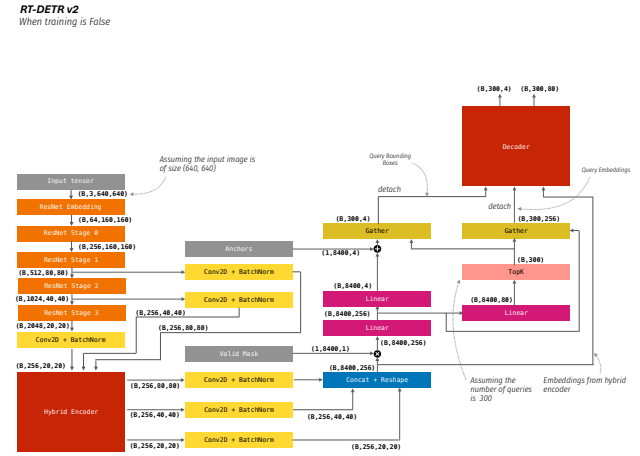


Figure 1: The structure of an RT-DETRv2 model with denoising task off.

2.1 CNN Backbone

The input image first passes through a ResNet-based embedding layer followed by several ResNet stages [5], producing three multi-scale feature maps of sizes $(B, 256, 80, 80)$, $(B, 256, 40, 40)$, and $(B, 256, 20, 20)$. These feature maps capture information at different spatial resolutions: the 80×80 map preserves fine-grained spatial detail but carries relatively shallow semantic context, whereas the 20×20 map provides coarse spatial resolution with richer semantic representation. The intermediate 40×40 map strikes a balance between the

two, supporting effective multi-scale feature integration in later stages of the model.

2.2 Hybrid Encoder

The hybrid encoder [6] consists of an encoder and a series of fusion pathways (Figure 2). The encoder performs self-attention [7] only on the feature map with lowest resolution and highest semantic richness to understand relationships and identify object features globally. The fusion pathways perform top-down and bottom-up feature aggregation [8] through the use of upsampling, downsampling, concatenation, and Cross-Stage Partial Networks [9] to ensure that high resolution features also contain deep semantic meaning.

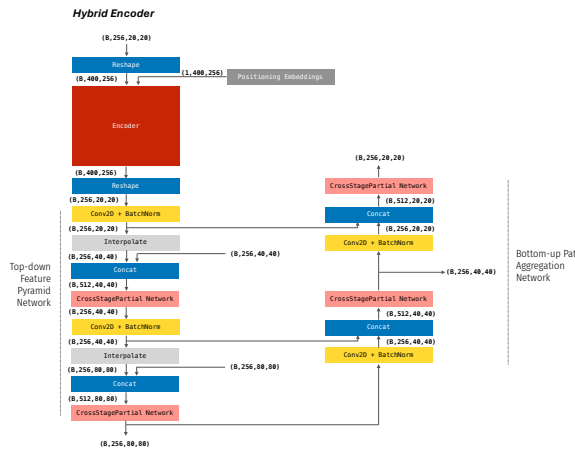


Figure 2: The structure of the hybrid encoder. The hybrid encoder is split into two distinct components: the encoder which performs normal self-attention, and the fusion pathways as seen by the Top-Down Feature Pyramid and Bottom-Up Path Aggregation Networks.

The Top-Down Feature Pyramid and Bottom-Up Aggregation Network are fusion pathways which aim to produce feature maps which are high in semantic richness and spatial resolution.

For the Top-Down Feature Pyramid, the $(B, 256, 20, 20)$ tensor is returned by the encoder and upsampled to size $(40, 40)$. It is concatenated with the $(B, 256, 40, 40)$ tensor from ResNet Stage 2 (Figure 1) resulting in 512 feature maps $(256 + 256)$. This is passed through a Cross Stage Partial (CSP) Network (Figure 3) to output a tensor of shape $(B, 256, 40, 40)$. The process repeats, where the tensor is upsampled and concatenated with the $(B, 256, 80, 80)$ feature maps from ResNet Stage 3 to result again in 512 feature maps. It is passed through another CSP Net to output a tensor of shape $(B, 256, 80, 80)$.

The Bottom-Up Path Aggregation Network operates similar to the Top-Down Feature Pyramid, just that it downsamples the tensors instead. The $(B, 256, 80, 80)$ tensor is then downsampled to size $(40, 40)$ and concatenated with the earlier $(B, 256, 40, 40)$ CSP Net output to produce a tensor with

512 maps. The tensor goes through the same process to output shape $(B, 256, 40, 40)$. These steps are repeated to output another tensor of shape $(B, 256, 20, 20)$. The resultant tensors of size $(80, 80)$, $(40, 40)$ and $(20, 20)$ each have 256 channels. These fused representations are the semantically and spatially rich outputs of the hybrid encoder for the rest of the model.

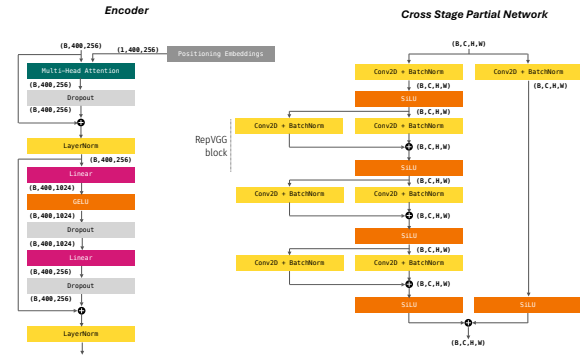


Figure 3: Left is the structure of the encoder, performing rather straightforward self-attention on the input tensor. Right is structure of the Cross Stage Partial Network which utilises RepVGG blocks [10] to allow for faster convergence and fewer vanishing gradients in deep neural networks.

2.3 Query Selection

The purpose of query selection is to reduce the dense set of candidate features into a smaller set of informative queries for the decoder. Once the $(B, 256, 80, 80)$, $(B, 256, 40, 40)$, and $(B, 256, 20, 20)$ feature maps have been returned by the hybrid encoder, they are concatenated and reshaped to a $(B, 8400, 256)$ tensor where 8400 represent the spatial locations across all scales and 256 represent the number of channels for each spatial location. A valid mask of shape $(1, 8400, 1)$ is then applied through element-wise multiplication to the tensor in order to omit any invalid spatial locations. The tensor is then passed through a linear layer to map feature embeddings to classification logits, resulting in shape $(B, 8400, 256)$.

Afterwards, the tensor is passed through a classification branch and a localisation branch. The classification branch passes the tensor through a linear layer resulting in $(B, 8400, 80)$ whereby the prediction ranges between 80 object classes. The $(B, 8400, 80)$ tensor is then passed through a TopK algorithm to gather the top 300 queries which likely contain important information to be input into the decoder.

The localisation branch is passed through a linear layer resulting in $(B, 8400, 4)$ where the last dimension represents the coordinates (x_1, y_1, x_2, y_2) . Anchors are added to the tensor at the localisation branch before the TopK queries are filtered out. Query selection ensures that only the most relevant queries are

forwarded to the decoder, reducing redundancy while preserving spatial diversity.

2.4 Denoising Task

When the denoising task [11] is enabled, the model takes certain ground truth images and labels and deliberately alters them slightly to create denoising queries. The denoising queries remove the need for matching since they directly correlate to the ground truth bounding boxes and labels. The denoising queries will have their own loss computed separately from the main queries.

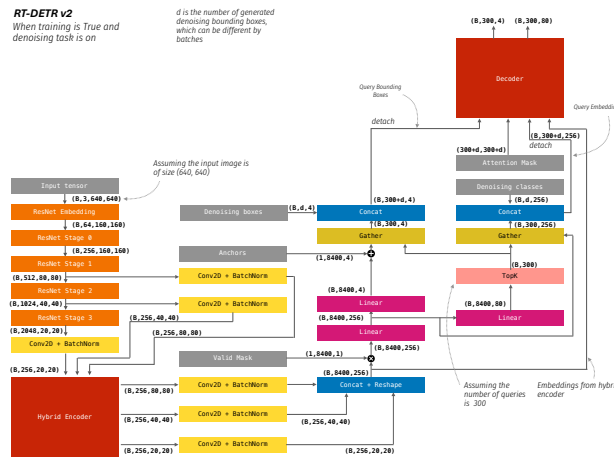


Figure 4: The structure of an RT-DETRv2 model with denoising task on.

2.5 Decoder

The decoder consists of six decoder blocks which takes the query embeddings, query bounding boxes, encoder embeddings, and attention masks as inputs which result in class and bounding box predictions as the output.

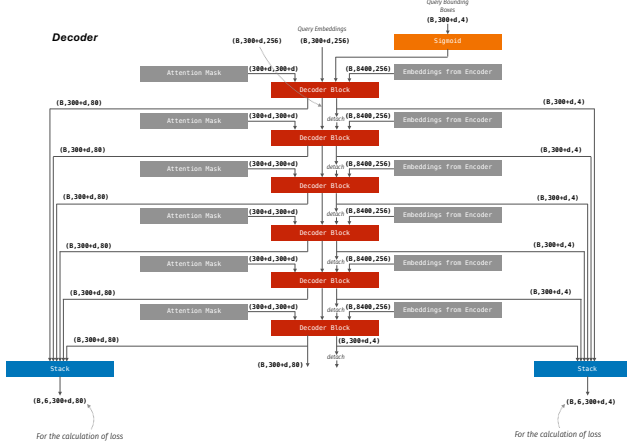


Figure 5: The structure of the decoder.

The decoder also has two stacks which compute the loss for each decoder block individually. The 'detach' label between each decoder block indicates that for bounding box prediction, there is no backpropagation through the decoder blocks, but rather gradient descent is directly computed from the loss stack for each individual block.

2.5.1 Decoder Block

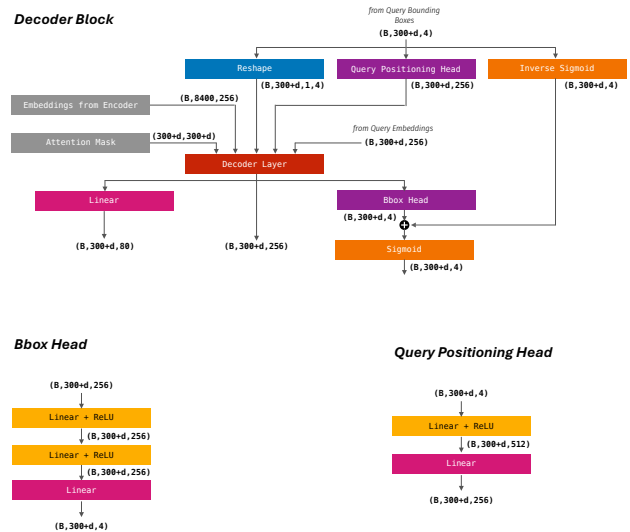


Figure 6: Above is the structure of the decoder block. Bottom left is the bbox head structure. Bottom right is the query positioning head structure.

Zooming in to the decoder block, the query bounding boxes are reshaped to $(B, 300 + d, 1, 4)$, where the additional dimension of 1 ensures compatibility with the computations required by multi-scale deformable attention. The inverse sigmoid is used to move bounding box coordinates from a bounded space of $[0, 1]$ to an unbounded space where the decoder can adjust the coordinates freely before passing it through the sigmoid function again to keep the prediction bounded.

The bbox head has the tensor pass through two linear + ReLU layers and a final linear layer to output a tensor of shape $(B, 300 + d, 4)$ with 4 coordinates per query. Since this is added element-wise with the output tensor of the inverse sigmoid function, the bbox head outputs positional offsets rather than the raw image coordinates, leading to a more precise result after the resultant tensor is passed through the sigmoid function.

The query positioning head has the tensor pass through a linear + ReLU layer to expand the tensor to a richer 512 dimensional representation before reducing it through a linear layer to the decoder's 256 dimensions.

2.5.2 Decoder Layer

The decoder layer is central to the decoder block as it processes the encoder embeddings, query embeddings, attention

mask, query bounding boxes, and query positional embeddings.

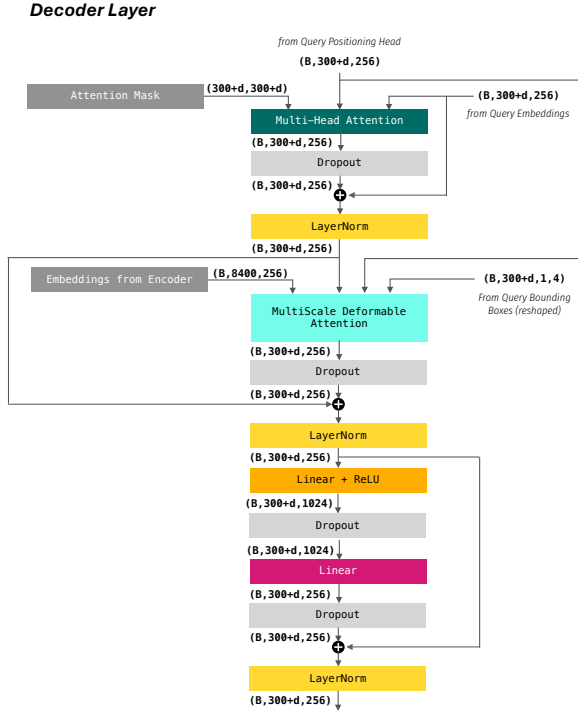


Figure 7: The structure of the decoder layer.

The decoder layer takes the tensors from the query positioning head ($B, 300 + d, 256$), query embeddings ($B, 300 + d, 256$) and the attention mask ($300 + d, 300 + d$), and put its through self-attention to refine the embeddings by exchanging contextual information, producing a tensor of shape ($B, 300 + d, 256$). The output is then passed through multi-scale deformable attention [12] where each query predicts a set of spatial reference points for the ($B, 8400, 256$) encoder feature map. The model then performs multi-scale deformable attention by attending only to the selected reference points, this selective attention allows for more precise detection since there is greater focus on areas of interest in the picture.

The output from the multi-scale deformable attention is added element-wise with the output from the query self-attention as a residual connection and passed through a feed-forward network to predict a tensor of (B , number of queries, embedding dimensions).

2.5.3 Multi-Scale Deformable Attention

In normal self-attention, each query computes similarity scores with all keys to determine attention weights. This global mechanism becomes computationally expensive for tasks in real-time object detection. In multi-scale deformable attention, the attention weights are instead learned through back-propagation.

In the default architecture with a ResNet-50 backbone, for each query (there are $300 + d$ of them when the denoising

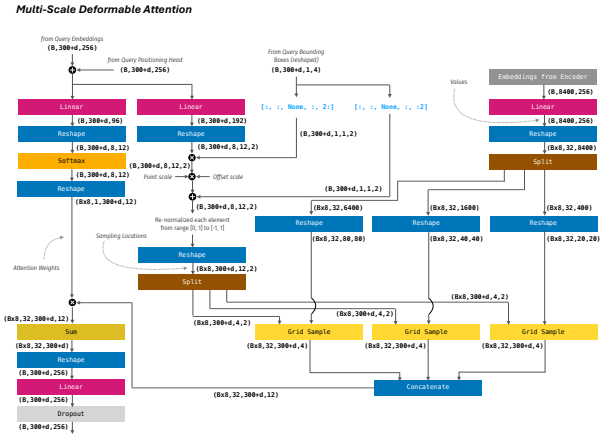


Figure 8: The structure for Multi-Scale Deformable Attention.

task is enabled), the total number of sampling locations to be attended to is 96: for each attention head, there are 4 sampling points, and there are 8 attention heads per scale, with a total of 3 scales. In Figure 8, this is reflected in the linear layer that transforms the tensor from shape ($B, 300 + d, 256$) to ($B, 300 + d, 96$).

On the other hand, the offsets for each sampling location (96 in total) are learned and produced by another linear layer. In Figure 8, this corresponds to the linear layer that transforms the tensor from shape ($B, 300 + d, 256$) to ($B, 300 + d, 192$), since each sampling location is represented by two values, x and y . The width and height of the query bounding boxes (in Figure 8, denoted by $[:, :, \text{None}, :, 2:]$) are involved in the process of generating these offsets. Each offset is then added to its corresponding query bounding box position, yielding the 96 sampling locations for each query bounding box. These sampling locations, now collated into a tensor of shape ($B, 300 + d, 8, 12, 2$), are re-normalized from the range $[0, 1]$ to $[-1, 1]$ a step required for the subsequent grid sampling computation.

On the encoder side, the output tensor of shape ($B, 8400, 256$) is reshaped and split into three tensors—each corresponding to one of the three scales. Each scale-specific feature map contains 32 channels per attention head (256/8). The sampling locations tensor is similarly split by scale, and grid sampling is applied to extract the values from the appropriate locations in each feature map. The sampled features across all scales are then concatenated along the point dimension, weighted by the attention weights, summed across sampling points, and reshaped to produce the output tensor of shape ($B, 300 + d, 256$). A final linear projection and dropout layer complete the operation.

3. CONCLUSION

RT-DETRv2 represents a powerful yet intricate architecture for real-time object detection. By unpacking the model step by step, we hope this article provides researchers and practition-

ers with a clearer understanding of how RT-DETRv2 works under the hood, and serves as a visual reference for future explorations into transformer-based object detection.

4. REFERENCES

- [1] Wenyu Lv, Yian Zhao, Qinyao Chang, Kui Huang, Guanzhong Wang, and Yi Liu. Rt-detr2: Improved baseline with bag-of-freebies for real-time detection transformer, 2024.
- [2] Joseph Redmon, Santosh Divvala, Ross Girshick, and Ali Farhadi. You only look once: Unified, real-time object detection, 2016.
- [3] Nicolas Carion, Francisco Massa, Gabriel Synnaeve, Nicolas Usunier, Alexander Kirillov, and Sergey Zagoruyko. End-to-end object detection with transformers, 2020.
- [4] Yian Zhao, Wenyu Lv, Shangliang Xu, Jinman Wei, Guanzhong Wang, Qingqing Dang, Yi Liu, and Jie Chen. Detrs beat yolos on real-time object detection, 2024.
- [5] Kaiming He, Xiangyu Zhang, Shaoqing Ren, and Jian Sun. Deep residual learning for image recognition, 2015.
- [6] Junhan Yang, Zheng Liu, Bowen Jin, Jianxun Lian, Defu Lian, Akshay Soni, Eun Yong Kang, Yajun Wang, Guangzhong Sun, and Xing Xie. Hybrid encoder: Towards efficient and precise native adsrecommendation via hybrid transformer encoding networks, 2021.
- [7] Ashish Vaswani, Noam Shazeer, Niki Parmar, Jakob Uszkoreit, Llion Jones, Aidan N. Gomez, Lukasz Kaiser, and Illia Polosukhin. Attention is all you need, 2023.
- [8] Tsung-Yi Lin, Piotr Dollár, Ross Girshick, Kaiming He, Bharath Hariharan, and Serge Belongie. Feature pyramid networks for object detection, 2017.
- [9] Chien-Yao Wang, Hong-Yuan Mark Liao, I-Hau Yeh, Yueh-Hua Wu, Ping-Yang Chen, and Jun-Wei Hsieh. Cspnet: A new backbone that can enhance learning capability of cnn, 2019.
- [10] Xiaohan Ding, Xiangyu Zhang, Ningning Ma, Jungong Han, Guiguang Ding, and Jian Sun. Repvgg: Making vgg-style convnets great again, 2021.
- [11] Feng Li, Hao Zhang, Shilong Liu, Jian Guo, Lionel M. Ni, and Lei Zhang. Dn-detr: Accelerate detr training by introducing query denoising, 2022.
- [12] Zhuofan Xia, Xuran Pan, Shiji Song, Li Erran Li, and Gao Huang. Vision transformer with deformable attention, 2022.